Desalination and Water Treatment
www.deswater.com
doi: 10.1080/19443994.2014.989913

57 (2016) 3995–4007
February

Taylor & Francis
Taylor & Francis Group

Removal of Ni(II) and Co(II) ions from aqueous solution using teak (*Tectona grandis*) leaves powder: adsorption kinetics, equilibrium and thermodynamics study

Sowmya Vilvanathan, S. Shanthakumar*

Environmental Engineering Division, School of Mechanical and Building Sciences, VIT University, Vellore 632014, India, Tel. +91 416 2202209; emails: sowmyavilvan@gmail.com (S. Vilvanathan), shanthakumar.s@vit.ac.in (S. Shanthakumar)

Received 19 March 2014; Accepted 14 November 2014

ABSTRACT

In the present study, batch experiments were carried out to elucidate the potential of teak leaves powder (TLP) to remove Ni(II) and Co(II) ions from aqueous solution. The TLP was characterized by Bruanauer, Emmett and Teller surface area, Fourier transform infrared spectroscopy and scanning electron microscopy. Effects of various process parameters such as initial pH (2–8), adsorbent dose (1–10 g L^{-1}), initial metal ion concentration (25–200 mg L^{-1}), contact time (5–120 min) and temperature (303–323 K) were investigated in their respective range and their optimum conditions were ascertained. Maximum percentage removal of 75.64 and 76.04% was achieved for Ni(II) and Co(II) ions, respectively, at an initial concentration of 50 mg L^{-1}, at their respective optimum pH of 6 and 5, adsorbent dose of 8 and 6 g L^{-1} in an equilibrium time of 30 and 60 min at 303 K. Adsorption kinetics was analyzed by pseudo-first-order, pseudo-second-order, Elovich and intraparticle diffusion kinetic models. It was found that the adsorption of both the metal ions followed pseudo-second-order kinetic model. Adsorption isotherms were modelled with Langmuir, Freundlich, Tempkin and Dubinin–Raduskevich models and their isotherm constants were calculated. The equilibrium data fitted well to the Langmuir isotherm model for adsorption of both Ni(II) and Co(II) ions on TLP. Thermodynamic parameters such as change in Gibb's free energy, change in enthalpy and change in entropy were calculated to predict the nature of adsorption process. The calculated thermodynamic parameters showed that the adsorption of Ni (II) and Co(II) ions on TLP were feasible, spontaneous and endothermic in nature.

Keywords: Adsorption; Teak leaves powder; Nickel; Cobalt; Kinetics; Isotherms; Thermodynamics

1. Introduction

Increasing population and rising demands have escalated the activities of industries all around the world. Intense activities of industries like metal electroplating, mining, mineral processing, battery manufacturing, electronics and petrochemicals, etc. have led to the release of heavy metals including nickel and cobalt, besides other forms of pollutants to the aquatic environment. The persistent and nonbiodegradable nature of these heavy metals demands its appropriate removal, which will otherwise pose a

*Corresponding author.

significant threat to the environment. Heavy metals, when left untreated can enter the microenvironment, the aquatic flora and fauna and in turn into the food chain and can show direct health effect on human beings.

Nickel is found naturally in the environment. Although nickel is an essential element for human nutrition at low concentration, it turns toxic at high levels of exposure. Nickel is used in the manufacture of nickel alloys, batteries, coins, stainless-steel, nickel–chrome resistance wires, and catalysts and in electroplating industries [1]. Acute exposure to nickel through inhalation leads to the damage of lungs and kidneys, gastrointestinal distress, neurotoxic effects, pulmonary fibrosis and renal edema. Its chronic exposure leads to dermatitis with symptoms of eczema and respiratory effects, including a type of asthma specific to nickel [2]. Cobalt is also a naturally occurring essential element in human beings, as a constituent of vitamin B_{12} [3]. However, at high concentration it is known to exhibit high risk to human life. Cobalt is used in the making of super-alloys and in pigment manufacture. Acute exposure to high levels of cobalt by inhalation results in respiratory effects, such as a significant decrease in ventilatory function, congestion and haemorrhage of the lungs. Chronic exposure to cobalt leads to respiratory irritation, cardiac and immunological effects [4].

Thus, the increased health risk associated with nickel and cobalt in the environment and its high level of discharge in the industrial wastewater streams necessitates immediate concern towards its removal or reduction. Several strategies have been applied in the treatment of heavy metal containing wastewater. Conventional methods including chemical precipitation, membrane filtration, ion-exchange, evaporation, solvent extraction and co-precipitation suffer severe disadvantages of being ineffective in treating effluents at low metal concentration, being expensive and uneconomical causing sludge disposal problems, etc. [5]. Adsorption technology in all aspects has taken advantage of being effective in treating heavy metals containing effluent, particularly for high volumes of dilute solution [6]. The ability to utilize low-cost agricultural wastes as adsorbents in the process is an added advantage for both economic and environmental reasons. Agricultural wastes are lignocellulosic biomaterials, containing high levels of cellulose, hemi cellulose and lignin [7] which provides a good potential for heavy metal adsorption. An annual estimate of 3.5×10^8 tons of agricultural biomass is disposed as solid waste [8]. Attempts to utilize these solid wastes as adsorbents for heavy metal removal have been carried out by many researchers [9–12] and they have shown good results. Agricultural wastes such as pomegranate peel [13], almond husk [14], barley straw [15], cashew nut shell [16], rice bran [17], watermelon rind [18], bagasse pith [19], banana stalk [20], hemp fibres [21], lemon peel [22] and many more have been used as adsorbents for the removal of nickel and cobalt ions from wastewater. Considering the abundant source of agro-wastes and its potential in removing different heavy metals, there is still a large sink of agricultural waste whose effectiveness is left unnoticed. This further necessitates the need to explore the potential of available natural agro-waste for their ability to remove heavy metals, which in turn can make a significant contribution in the field of environmental protection.

Plant leaves, an important agricultural waste with abundant availability are often disposed as waste, despite their rich lignocellulosic structural components which are known for effective heavy metal adsorption. Teak leaves contain cellulose, hemicellulose, lignin and tannin as their cell wall components with carboxyl, hydroxyl and oxyl groups as functional sites, which shows good potential in adsorbing heavy metals [23]. Hence, in the present study, teak (*Tectona grandis*) leaves have been chosen as an adsorbent for the removal of Ni(II) and Co(II) ions from aqueous solutions. Adsorption studies were carried out for the removal of nickel and cobalt ions using teak leaves in their native state. The main objective of this study includes: (1) characterization of teak leaves powder (TLP) through Brunauer, Emmett and Teller (BET) surface area analysis, scanning electron microscopy (SEM) and Fourier transform infrared (FTIR) spectroscopy analysis, (2) the study of effect of different process parameters: initial pH, adsorbent dosage, initial metal ion concentration with contact time and temperature on the removal of Ni(II) and Co(II) ions from aqueous solution, (3) analysis of the experimental data with various kinetics and isotherm models to find out the best fit and (4) assessment of the thermodynamic parameters as a function of temperature.

2. Materials and methods

2.1. Preparation of adsorbent

Dry teak leaves were collected from the locales of Vellore district (Tamil Nadu, India). The leaves were washed thoroughly 3–4 times in tap water to remove dust and other impurities adhered to it. It was then dried in a hot air oven at 80˚C for 12 h. The dried leaves were ground to fine powder using a domestic mixer. The powdered teak leaves were washed with double distilled water and dried in an oven at 80˚C

Table 1
Physical properties of TLP

Parameter	Value
Moisture content (%)	8.09
Volatile matter (%)	30.75
Ash content (%)	30.82
Fixed carbon content (%)	30.32
Bulk density (g/cc)	0.47

for 24 h. The prepared TLP were cooled in desiccators and sieved to desired particle size (<90 μm) and was further used as adsorbent. Table 1 presents the physical properties of TLP.

2.2. Preparation of stock solution

Stock solution of 1,000 mg L^{-1} concentration of Ni (II) and Co(II) ions were prepared by dissolving 4.785 and 4.037 g of $NiSO_4{\cdot}7H_2O$ and $CoCl_2{\cdot}6H_2O$, respectively, in 1,000 ml of double distilled water. All working solutions of varying concentrations were obtained by successive dilution of the above stock solutions. The pH of the solution was adjusted to the desired value with 0.1 M H_2SO_4 and 0.1 M NaOH. All chemicals used in this work were of analytical reagent grade and were used without any further purification.

2.3. Adsorption experiments

Batch adsorption experiments were carried out to investigate the effect of initial pH, adsorbent dose, initial metal ion concentration, contact time and temperature on the adsorption of Ni(II) and Co(II) ions on TLP by varying the parameter under study and keeping the other parameters as constant. Each experiment was carried out in 250 ml conical flasks with 100 ml aqueous solution of known metal ion concentration and adsorbent dosage. The reaction mixture was agitated at 150 rpm in an orbital incubating shaker (REMI, CSI 24BL) at the desired temperature. The effect of pH (2–8), adsorbent dosage (1–10 g L^{-1}), initial metal ion concentration (25–200 mg L^{-1}), contact time (5–120 min) and temperature (303–323 K) in their respective range were separately studied each for Ni (II) and Co(II) ions adsorption on TLP. The analysis of sample was done after filtering it using Whatmann No. 1 filter paper. The concentrations of Ni(II) and Co (II) ions in the filtrates were analyzed using flame atomic absorption spectrophotometer (Varian, AA240). The percentage removal of Ni(II) and Co(II) ions from aqueous solution was calculated using Eq. (1):

$$\%\ \text{removal} = \frac{(C_0 - C_e)}{C_0} \times 100 \tag{1}$$

where C_0 and C_e are the initial and equilibrium metal ion concentration (mg L^{-1}), respectively.

2.4. Adsorption kinetics

Adsorption kinetics studies were conducted to determine the influence of contact time on metal ion adsorption at different initial metal ion concentrations (25–200 mg L^{-1}) of Ni(II) and Co(II) ions at their respective optimum pH and adsorbent dose at 303 K. The experimental data were applied to different kinetic models namely, pseudo-first-order kinetics, pseudo-second-order kinetics, Elovich and intraparticle diffusion models. Samples were analyzed at pre-determined time intervals (5–120 min) and the amount of metal ion adsorbed at time t, q_t (mg g^{-1}), was calculated by the following expression, Eq. (2):

$$q_t = \frac{(C_0 - C_t)V}{m} \tag{2}$$

where C_t is the concentration of metal ion at time, t (mg L^{-1}), V is the volume of the solution (L) and m is the mass of the adsorbent (g).

2.5. Adsorption isotherms

Adsorption equilibrium studies were carried out for different initial concentrations (25–200 mg L^{-1}) of Ni(II) and Co(II) ions at varying temperature (303–323 K) to determine the applicability of Langmuir, Freundlich, Temkin and Dubinin–Radushkevich (D–R) adsorption isotherm models under the respective optimum conditions of initial pH, adsorbent dose and equilibrium time. The amount of metal ion adsorbed at equilibrium was determined using the following expression:

$$q_e = \frac{(C_0 - C_e)V}{m} \tag{3}$$

where q_e is the quantity of metal ion adsorbed at equilibrium time (mg g^{-1}).

2.6. Adsorbent characterization

The specific surface area of adsorbent was determined using BET method (Micromeritics ASAP2020 Porosimeter). Surface structure and morphology of

TLP before and after adsorption of Ni(II) and Co(II) ions were investigated using scanning electron microscope (FEI Quanta FEG200 HR-SEM). FTIR studies on TLP before and after adsorption of metal ions were carried out using FTIR spectrometer (Thermo Nicolet, AVATAR 330) to identify the functional groups responsible for adsorption. The sample prepared as KBr disc was examined over the wave number in a range of 4,000–400 cm^{-1}.

3. Results and discussion

3.1. Characterization of TLP

3.1.1. BET surface area

The specific surface area of the adsorbent was evaluated from the N_2 adsorption isotherms by applying the BET equation in the relative pressure (P/P_o) range between 0.04 and 0.11 [24]. BET surface area of TLP was found to be 0.959 $m^2 g^{-1}$. Similar results have been found in other agro-waste adsorbents like rice husk (0.918 $m^2 g^{-1}$) [25] and *Uncaria gambir* plant (0.970 $m^2 g^{-1}$) [26].

3.1.2. SEM micrographs

The SEM micrographs of raw TLP, Ni(II)-loaded TLP and Co(II)-loaded TLP are presented in Fig. 1(a)–(c), respectively. It can be observed from Fig. 1(a) that raw TLP has asymmetric pores and an open pore structure which can provide suitable binding sites for the adsorption of Ni(II) and Co(II) ions. Fig. 1(b) and (c) presents the SEM micrographs of TLP after the adsorption of Ni(II) ions and Co(II) ions, respectively.

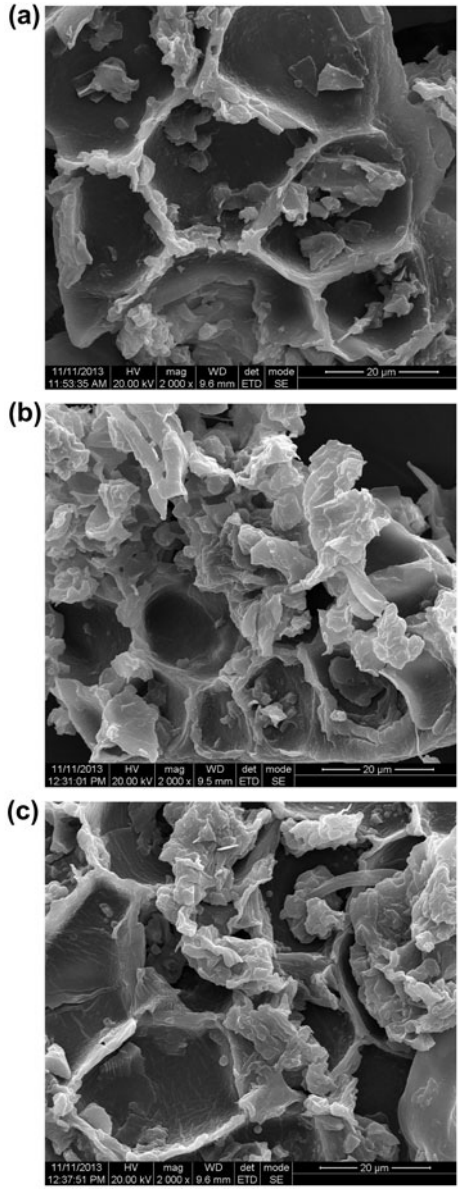

Fig. 1. SEM micrographs of (a) raw TLP, (b) Ni(II)-loaded TLP and (c) Co(II)-loaded TLP.

3.1.3. FTIR analysis

The FTIR spectra were used to examine the vibrational frequency changes of functional groups that were involved in the adsorption process. Fig. 2 depicts the infrared spectra of raw TLP (a), Ni(II)-loaded TLP (b) and Co(II)-loaded TLP (c). The presence of many functional groups in the spectra indicated the complex nature of TLP. In Fig. 2(a), a broad band at 3,198 cm^{-1} indicated the presence of hydroxyl groups, a strong peak at 2,918 cm^{-1} is due to the C–H stretching frequency and the peak at 1,608 cm^{-1} is due to N–H bending of the primary amines. A peak at 1,404 cm^{-1} corresponds to C–OH bending and a strong peak at 1,062 cm^{-1} is due to C–O stretching mode. In Fig. 2(b) and (c), a strong band at 3,423 and 3,439.08 cm^{-1} corresponds to O–H stretching which indicates a downward shift in the absorption frequency after the adsorption of Ni(II) and Co(II) ions, respectively. After the adsorption of Ni(II) and Co(II) ions, there was a shift in the absorption frequencies from 2,918 cm^{-1} to 2,916 cm^{-1} and 2,922 cm^{-1}, respectively, in the C–H stretching region. An upward shift was observed in the N–H stretching region from 1,608 to 1,612 and 1,631 cm^{-1}, respectively, for Ni(II)- and Co(II)-adsorbed TLP. Another shift in the C–O stretching region was observed in the infrared spectra of TLP after the adsorption of Ni(II) and Co(II) at 1,064 and 1,072 cm^{-1}, respectively [27]. The interpretation of the

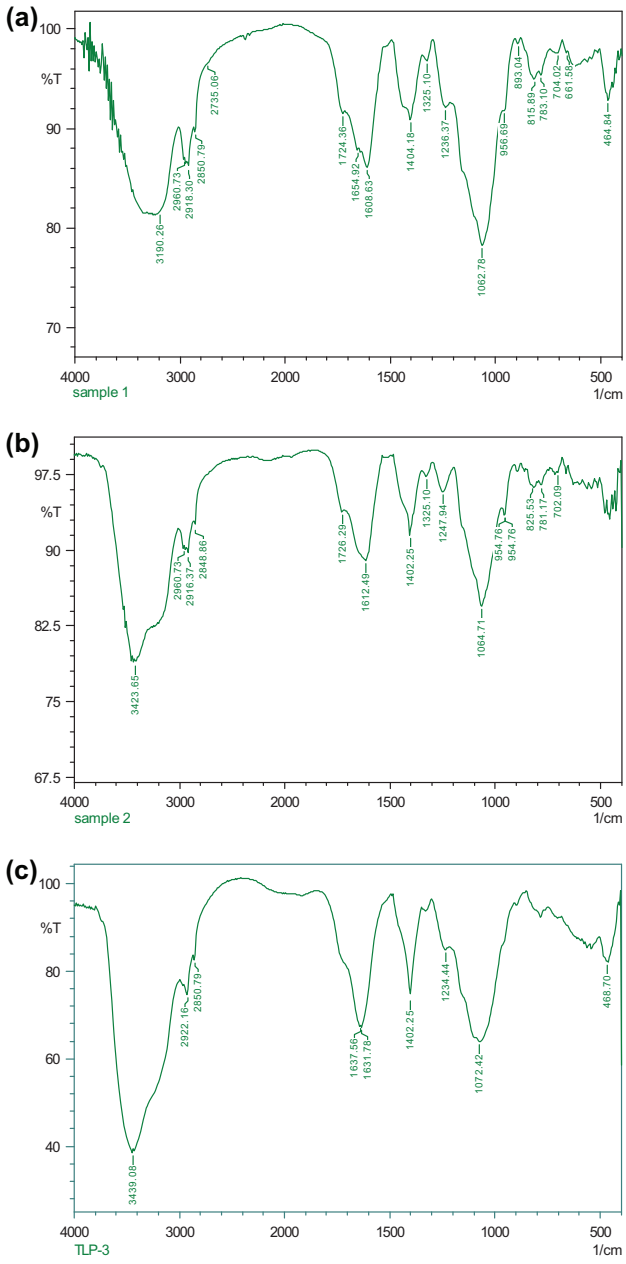

Fig. 2. FTIR spectra of (a) raw TLP, (b) Ni(II)-loaded TLP and (c) Co(II)-loaded TLP.

spectra indicated the interaction of hydroxyl, carboxyl and amine functional groups in the adsorption of Ni (II) and Co(II) ions on TLP.

3.2. Effect of initial pH

The pH is an important factor controlling the adsorption process since it substantially affects the mechanism of metal ion uptake. It also governs the speciation of metal ions and the dissociation of active sites on the adsorbent [28]. Batch adsorption experiments were carried out by varying the initial pH in the range of 2–8 to determine the effect of pH on the removal of Ni(II) and Co(II) ions from aqueous solution by TLP. The results are shown in Fig. 3. It can be observed from the figure that the percentage removal of metal ions steadily increased with increasing initial pH and reached a maximum at pH 6 and pH 5 for Ni(II) and Co(II) ions, respectively, and decreased later. The lower percentage removal at low pH is apparently due to the higher concentration of H^+ ions in the solution which competes with Ni(II) and Co(II) ions for the active adsorption sites on TLP. However, with increasing pH, the concentration of H^+ ions decreases which leads to the increased uptake of Ni(II) and Co(II) ions. The further decrease in the removal percentage at pH (>6) for Ni(II) ions and pH (>5) for Co(II) ions was due to the formation of their respective soluble metal hydroxide complexes which decreases the free metal ion concentration in the aqueous solution. Similar observations have been reported in the literature for nickel and cobalt ion removal from aqueous solution [21,29]. Accordingly, further investigations were carried out at pH 6 and 5 as optimum initial pH for removal of Ni(II) and Co(II) ions, respectively.

3.3. Effect of adsorbent dosage

Adsorbent dose is an important parameter as it determines the adsorptive capacity of the adsorbent. Experiments were carried out to determine the effect of adsorbent dose in the range of 0.1–1 g (100 ml)$^{-1}$ for the removal of Ni(II) and Co(II) ions from their respective aqueous solution. From Fig. 4, it can be observed that the removal of metal ions increased with increasing adsorbent dose, however, beyond the adsorbent dose of 0.8 g (100 ml)$^{-1}$ and 0.6 g (100 ml)$^{-1}$ for Ni(II) and Co(II) ions, respectively, the percentage removal almost remained a constant which could be due to the

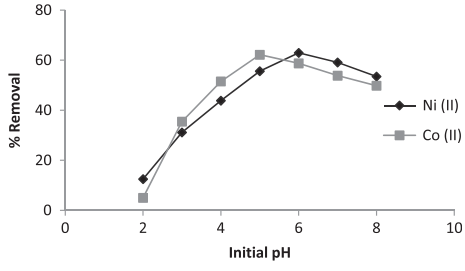

Fig. 3. Effect of pH on the adsorption of Ni(II) and Co(II) ions on TLP (working conditions: adsorbent dose—0.3 g (100 ml)$^{-1}$; initial metal ion conc.—50 mg L^{-1}; contact time —60 min; temp—30 °C; stirring speed—150 rpm).

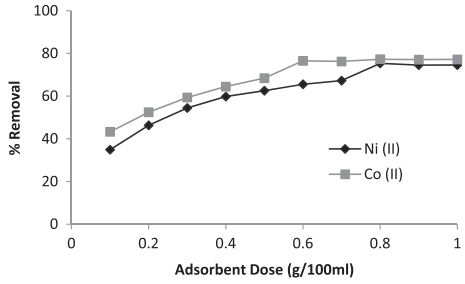

Fig. 4. Effect of adsorbent dose on the adsorption of Ni(II) and Co(II) ions (working conditions: initial pH 6.0 for Ni(II) and pH 5.0 for Co(II); initial metal ion conc.—50 mg L^{-1}; contact time—60 min; temp—30°C; stirring speed—150 rpm).

attainment of equilibrium in the adsorption system [30]. The initial increasing trend can be attributed to the availability of more active sites with increasing adsorbent dose [31]. Hence, an optimum TLP dose of 0.8 g (100 ml)$^{-1}$ for Ni(II) and 0.6 g (100 ml)$^{-1}$ for Co (II) ions was considered for rest of the experiments.

3.4. Effect of initial metal ion concentration with contact time

Initial metal ion concentration provides an important driving force to overcome all the mass transfer resistances which exists in the adsorption system [32]. Effect of varying initial metal ion concentration (25, 50, 100, 150, 200 mg L^{-1}) was studied over a range of varying contact time (5, 10, 15, 30, 45, 60, 90, 120 min) for both Ni(II) (Fig. 5) and Co(II) ions (Fig. 6) in the aqueous solution. It can be observed from Figs. 5 and 6 that the percentage removal decreases with increasing initial metal ion concentration. This may be due to the fact that, at low concentration, the ratio of available surface binding sites to the initial metal ion concentration is large, and it enhances removal. However, as the metal concentration increases, this ratio decreases and hence leads to less percentage

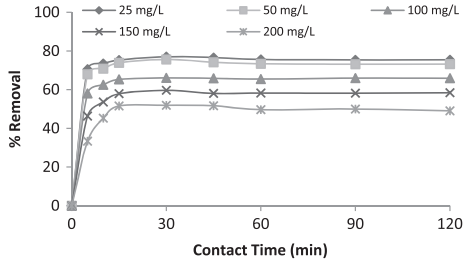

Fig. 5. Effect of initial Ni concentration with contact time (working conditions: initial pH 6.0; adsorbent dose—0.8 g (100 ml)$^{-1}$; temp—30°C; stirring speed—150 rpm).

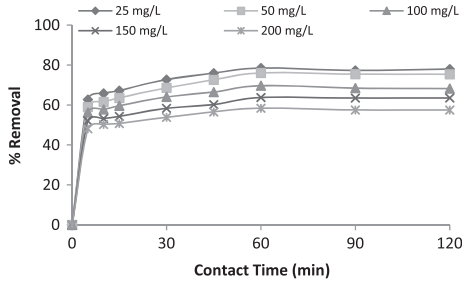

Fig. 6. Effect of initial Co concentration with contact time (working conditions: initial pH 5.0; adsorbent dose—0.6 g (100 ml)$^{-1}$; temp—30°C; stirring speed—150 rpm).

removal [33]. But, the adsorption capacity (q_e) increases as initial metal ion concentration increases. This increase in metal uptake capacity may be due to the increasing driving force i.e. as the concentration increases the gradient overcomes all mass transfer resistance between the solid and aqueous phases [21]. Thus, it can be concluded that the metal ion removal was concentration dependent. Similar trends have also been reported in the literature [16].

From Figs. 5 and 6, it can also be noted that the removal of metal ions were very rapid in the initial period of contact time, and thereafter it decreased gradually and reached a maximum at the equilibrium point, which was observed as 30 min for Ni(II) and 60 min for Co(II) ions. The equilibrium time is found to be the same for all different concentrations studied and hence, an equilibrium time of 30 and 60 min are considered for Ni(II) and Co(II) ions, respectively, for all further studies.

3.5. Adsorption kinetics

Adsorption kinetics reveals the mechanism of adsorption and its potential rate-limiting step which include mass transfer and surface reaction processes [34]. The adsorption kinetics of Ni(II) and Co(II) ions on TLP were investigated as a function of contact time at different initial metal ion concentrations (25–200 mg L^{-1}). In this study, four different kinetic models, namely pseudo-first-order model, pseudo-second-order model, Elovich's kinetic model, and Weber and Morris's intraparticle diffusion model, have been employed to understand the adsorption kinetics and to quantify the rate of adsorption.

3.5.1. Pseudo-first-order model

The pseudo-first-order kinetic model as proposed by Lagergren assumes that the adsorption process is first-order in nature and is dependent only on the

number of metal ions present at a specific time in the solution. The rate equation of the pseudo-first-order model is expressed as Eq. (4) [35]:

$$\log(q_e - q_t) = \log q_e - \frac{K_1}{2.303} \cdot t \quad (4)$$

where q_e and q_t are the amount of metal adsorbed (mg g^{-1}) at equilibrium and at time, t (min), respectively, and K_1 is the rate constant of pseudo-first-order reaction (min^{-1}). The values of K_1 and $q_{e(cal)}$ were determined from the slope and intercept of the plot of log ($q_e - q_t$) versus time. Fig. 7(a) and (b) depicts the plot of different kinetic models for the adsorption of Ni(II) and Co(II) ions on TLP, respectively, at 50 mg L^{-1} initial metal ion concentration. The values of K_1, the calculated adsorptive capacity ($q_{e(cal)}$) and correlation coefficient (R^2) for both Ni(II) and Co(II) ions were presented in Table 2. It can be noted from Table 2 that the theoretical $q_{e(cal)}$ values calculated from the pseudo-first-order model did not agree well with the experimental values $q_{e(exp)}$ and hence, the adsorption process does not follow the pseudo-first-order model for both the metal ions.

3.5.2. Pseudo-second-order model

The pseudo-second-order model assumes that the metal adsorption is dependent both on the number of metal ions present in the solution and the free adsorption sites on the adsorbent surface. The pseudo-second-order kinetic rate equation is expressed as Eq. (5) [36,37]:

$$\frac{t}{q_t} = \frac{1}{K_2 \cdot q_e^2} + \frac{1}{q_e}(t) \quad (5)$$

where K_2 is the rate constant of pseudo-second-order adsorption (g mg^{-1} min^{-1}). The values of $q_{e(cal)}$ and K_2 were calculated from the slope and intercept of the linear plot of t/q_t versus time. The values of pseudo-second-order kinetic constants along with the corresponding correlation coefficients (R^2) were presented in Table 2. It can be noted from Table 2 that the theoretical values $q_{e(cal)}$ agree well with the experimental values $q_{e(exp)}$. Further, the correlation coefficient values (R^2) were observed as ≅0.99 for both the metal ions suggesting that the adsorption process can be more favourably described by pseudo-second-order kinetic model.

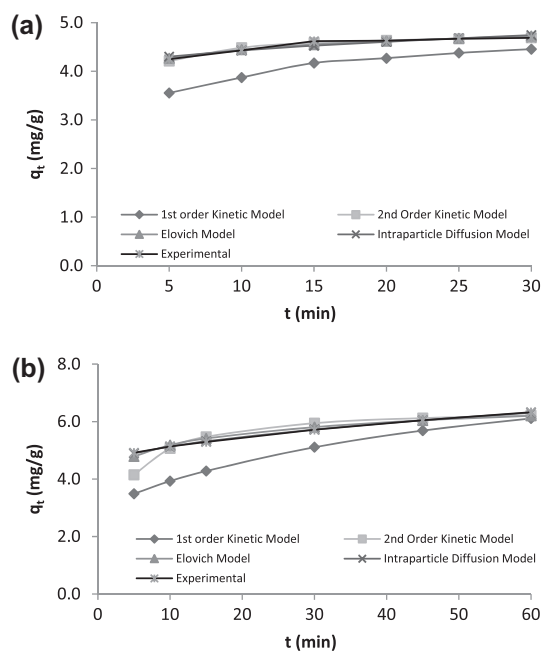

Fig. 7. Kinetic models of (a) Ni(II) and (b) Co(II) adsorption on TLP (for C_0 = 50 mg L^{-1}).

3.5.3. Elovich's kinetic model

Elovich's kinetic model gives a rate equation based on the adsorption capacity of the adsorbent. The rate equation of Elovich's kinetic model is expressed as Eq. (6) [38]:

$$q_t = \frac{1}{\beta} \cdot \ln(\alpha\beta) + \frac{1}{\beta} \cdot \ln t \quad (6)$$

where α is the initial adsorption rate (mg g^{-1} min^{-1}), β is the desorption constant related to the extent of surface coverage and activation energy for chemisorption (g mg^{-1}). The values of Elovich kinetic constants, α and β were obtained from the intercept and slope of the plot of q_t versus ln t and were presented in Table 2. It can be inferred from Table 2 that the correlation coefficient values (R^2) was less compared to that of pseudo-second-order model for both the metal ions, proving the inapplicability of this model to this adsorption system.

3.5.4. Weber and Morris's intraparticle diffusion model

The kinetic data was further analyzed using the intraparticle diffusion model based on the theory proposed by Weber and Morris [22,39]. The rate equation of intraparticle diffusion model is expressed as Eq. (7):

$$q_t = K_{dif} \cdot t^{0.5} + C \quad (7)$$

Table 2
Adsorption kinetics parameters for Ni(II) and Co(II) adsorption by TLP

			Adsorption kinetic models											
			Pseudo-first-order			Pseudo-second-order			Elovich model			Intraparticle diffusion		
Metal ion	Metal ion conc. (mg L^{-1})	qe (exp.) (mg g^{-1})	K_1 (min^{-1})	q_e (calc.) (mg g^{-1})	R^2	K_2 (gm g^{-1} min^{-1})	q_e (calc.) (mg g^{-1})	R^2	α (mg g^{-1} min^{-1})	β (g mg^{-1})	R^2	$K_{dif.}$ (mg g^{-1} $min^{-0.5}$)	C (mg g^{-1})	R^2
Ni(II)	25	2.408	0.111	2.946	0.966	0.718	2.440	0.999	20,432,744	9.325	0.968	0.057	2.103	0.910
	50	4.727	0.100	1.405	0.960	0.298	4.798	0.999	943,665.3	3.921	0.952	0.136	3.996	0.897
	100	8.263	0.222	3.585	0.974	0.147	8.503	0.999	47,384.0	1.756	0.916	0.299	6.783	0.832
	150	11.193	0.131	3.881	0.954	0.053	11.754	0.999	197.68	0.735	0.918	0.714	7.560	0.835
	200	12.984	0.220	8.561	0.882	0.024	14.461	0.994	16.850	0.384	0.860	1.347	6.458	0.760
Co(II)	25	3.271	0.055	1.016	0.967	0.133	3.334	0.999	973.29	3.821	0.980	0.117	2.363	0.993
	50	6.336	0.079	3.368	0.823	0.054	6.508	0.997	514.57	1.757	0.961	0.257	4.318	0.999
	100	11.614	0.053	3.652	0.921	0.037	11.787	0.998	5,578.81	1.131	0.962	0.399	8.425	0.996
	150	15.943	0.064	5.963	0.816	0.026	16.173	0.997	14,464.15	0.873	0.931	0.523	11.689	0.986
	200	19.468	0.070	6.980	0.867	0.024	19.840	0.998	32,108.0	0.739	0.959	0.611	14.679	0.994

where K_{dif} is the intraparticle diffusion rate constant (mg g^{-1} $min^{0.5}$), C is the intercept (mg g^{-1}). The values of K_{dif} and C were calculated from the slope and intercept of the plot of q_t versus $t^{0.5}$ and are presented in Table 2. The value of C gives an idea about the thickness of boundary layer (as the intercept increases, the resistance to external mass transfer increases). From Table 2, it can be noted that the R^2 values for Co(II) ions are close to unity which suggests that intraparticle diffusion plays a significant role in the adsorption of Co(II) ions by TLP. However, if intraparticle diffusion has to be the sole rate-limiting step, the plots of q_t versus $t^{0.5}$ should pass through the origin [40], but the present study for Co(II) adsorption on TLP deviates from the requirement and hence the adsorption process does not follow the intraparticle diffusion model.

Based on the kinetic studies for the adsorption of Ni(II) and Co(II) ions on TLP, it was found that though the $q_{t(calc)}$ and $q_{t(exp)}$ for both the ions correlated well for pseudo-second-order, Elovich and intraparticle diffusion models (Fig. 7), the limitations of each model and the deviation in correlation co-efficient (R^2) values suggest the inapplicability of Elovich and intraparticle diffusion model. Hence, pseudo-second-order kinetic model is considered more appropriate to represent the kinetic data for the adsorption of Ni(II) and Co(II) ions on TLP. This indicates, chemisorption involving exchange of electrons between adsorbate and adsorbent, complexation and/or chelation to be the rate-limiting step.

3.6. Adsorption isotherm

Adsorption isotherms represent the distribution of the solute at equilibrium between the solid phase (q_e) and the liquid phase (C_e). The adsorption of Ni(II) and Co(II) ions on TLP was carried out at different temperatures (303–323 K) for different initial metal ion concentrations (25–200 mg L^{-1}) at 150 rpm at their respective optimum pH, adsorbent dose and equilibrium time. Analysis of isotherm data is important in the study and design of adsorption systems. Langmuir and Freundlich isotherm models are the most widely used surface adsorption models for single-solute systems. In this study, the experimental data were analyzed with Langmuir, Freundlich, Temkin and D–R isotherm equations.

3.6.1. Langmuir isotherm

The Langmuir model assumes monolayer adsorption onto a homogenous surface without interaction with the other adsorbed molecules. It also assumes uniform energy of adsorption onto the surface and allows no transmigration. The linear form of Langmuir equation is expressed as Eq. (8) [41]:

$$\frac{C_e}{q_e} = \frac{1}{K_1 \cdot Q_m} + \frac{C_e}{Q_m} \tag{8}$$

where q_e is the amount of metal ion adsorbed per unit weight of adsorbent (mg g^{-1}), C_e is the equilibrium concentration of metal ion in the solution (mg L^{-1}), Q_m is the monolayer adsorption capacity (mg g^{-1}) and K_l is the constant related to the free energy of adsorption. The Langmuir isotherm constants, Q_m and K_1 (Table 3) were obtained from the slope and intercept of the plot of C_e/q_e versus C_e. Fig. 8(a) and (b) depicts the plot of different isotherm models for the adsorption of Ni(II) and Co(II) ions using TLP at 303 K. It can be seen from Table 3, that maximum monolayer capacity, Q_m of 17.81 and 29.48 mg g^{-1} was obtained for the adsorption of Ni(II) and Co(II) ions by TLP, respectively, at 303 K. Further, the high correlation coefficient values (R^2) obtained for both the metal ions suggest that the adsorption process can be more favourably described by Langmuir isotherm model.

The feasibility of the Langmuir isotherm is described in terms of a dimensionless constant, separation factor (R_L). If this value lies in between 0 and 1, then the adsorption process is favourable. Separation factor, R_L is calculated using the following expression, Eq. (9) [42]:

$$R_L = 1 + \frac{1}{K_1 C_0} \tag{9}$$

From Table 3, it can be noted that all the experimental data obtained from this study were lying between 0 and 1, which indicates favourable adsorption.

3.6.2. Freundlich isotherm

The Freundlich isotherm assumes adsorption on a heterogeneous surface. The linear form of the equation is expressed as Eq. (10) [43]:

$$\log q_e = \log K_f + \frac{1}{n} \log C_e \tag{10}$$

where K_f is a constant which indicates the relative adsorption capacity of the adsorbent (mg g^{-1}) and n is an empirical parameter that indicates the intensity of adsorption. The Freundlich isotherm constants are obtained by plotting log q_e versus log C_e (Table 3).

Table 3
Adsorption isotherm parameters for Ni(II) and Co(II) adsorption by TLP

Metal ion	Temperature (K)	Adsorption isotherm models													
		Langmuir isotherm				Freundlich isotherm			Tempkin isotherm			D–R isotherm			
		Q_m (mg g^{-1})	K_l (L mg^{-1})	R^2	R_L	n	K_f (mg g^{-1})	R^2	B_T (mg L^{-1})	A_T (L g^{-1})	R^2	$K_{D-R} \times 10^{-6}$ (mol^2 kJ^{-2})	Q_m (mg g^{-1})	R^2
Ni(II)	303	17.809	0.027	0.997	0.153	1.690	0.960	0.978	3.781	0.302	0.992	9.362	10.510	0.941
	313	17.572	0.030	0.997	0.141	1.734	1.043	0.982	3.731	0.331	0.991	7.412	10.697	0.944
	323	18.112	0.032	0.997	0.134	1.737	1.115	0.979	3.839	0.353	0.993	6.280	11.338	0.959
Co(II)	303	29.485	0.0224	0.996	0.181	1.539	1.181	0.990	5.910	0.277	0.981	8.724	15.192	0.933
	313	27.505	0.028	0.987	0.151	1.646	1.432	0.984	5.634	0.333	0.982	6.452	16.010	0.949
	323	27.215	0.031	0.981	0.136	1.711	1.624	0.993	5.520	0.383	0.973	4.436	16.407	0.944

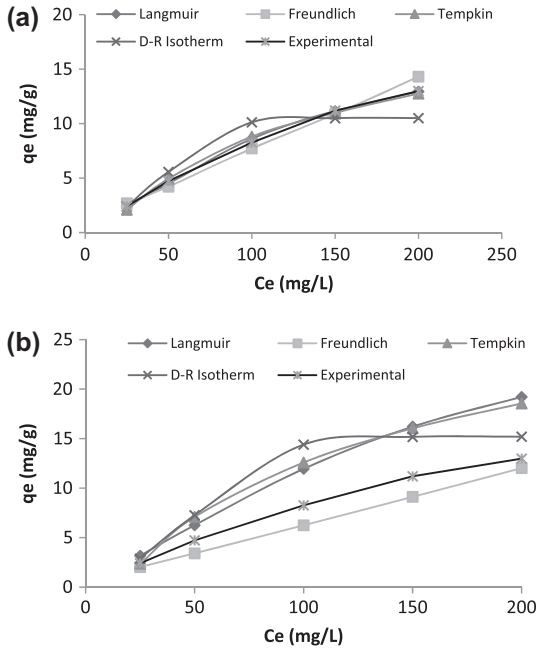

Fig. 8. Isotherm model of (a) Ni(II) and (b) Co(II) adsorption on TLP (at T = 303 K).

3.6.3. Temkin isotherm

Temkin isotherm assumes that, due to the adsorbate–adsorbate repulsions, the heat of adsorption of all the molecules in the layer decreases linearly with the coverage of molecules and the adsorption of adsorbate is uniformly distributed. The Temkin isotherm is expressed as Eq. (11) [44]:

$$q_e = B_T \ln A_T + B_T \ln C_e \tag{11}$$

where B_T is related to the heat of adsorption and A_T corresponds to the maximum binding energy. B_T and A_T can be determined by a plot of q_e versus ln C_e. The Temkin isotherm constants along with their correlation coefficient values (R^2) are presented in Table 3.

3.6.4. D–R isotherm

The D–R isotherm model estimates the characteristic porosity and the apparent free energy of adsorption. The linear form of the D–R model is expressed as Eq. (12) [44]:

$$\ln q_e = \ln Q_m - K_{D-R}\varepsilon^2 \tag{12}$$

where K_{D-R} is the constant related to the adsorption energy, Q_m is the theoretical monolayer saturation

Table 4
Thermodynamic parameters for Ni(II) and Co(II) adsorption by TLP

Metal ion	Temperature (K)	Thermodynamic parameters			
		$-\Delta G^\circ$ (kJ mol^{-1})	ΔS° (J mol^{-1} K^{-1})	ΔH° (kJ mol^{-1})	R^2
Ni(II)	303	1.036	31.787	10.652	0.993
	313	0.670			
	323	0.402			
Co(II)	303	1.786	16.705	6.855	0.996
	313	1.641			
	323	1.451			

capacity (mg g−1) and ε is the Polanyi potential calculated from Eq. (13)

$$\varepsilon = RT \ln\left(1 + \frac{1}{C_e}\right) \tag{13}$$

The slope and intercept of the plot of ln q_e versus ε^2 gives the constant values K_{D-R} (mol^2 kJ^{-2}) and Q_m (mg g^{-1}), respectively (Table 3). It can be inferred from Table 3 that, the correlation coefficients obtained from this model are lower, suggesting the inapplicability of this model.

Based on the equilibrium modelling of Ni(II) and Co(II) ion removal using TLP, it can be concluded that the values obtained from Langmuir isotherm model agreed well with the experimental data and had higher correlation co-efficient (R^2) values compared to other models tested, suggesting that the adsorption of Ni(II) and Co(II) ions on TLP can be best described by Langmuir isotherm model.

3.7. Adsorption thermodynamics

The effect of temperature on adsorption of Ni(II) and Co(II) ion on TLP were investigated at different temperatures (303, 313 and 323 K) with varying initial metal ion concentrations (25–200 mg L^{-1}) at their optimum pH and adsorbent dose. It was observed that the percentage removal of both the ions increase with increase in temperature and decrease with increase in initial metal ion concentration. Different thermodynamic parameters such as Gibbs free energy change (ΔG°), the standard enthalpy (ΔH°) and the standard entropy (ΔS°) were determined for better understanding of the adsorption process [45]. The Gibbs free energy change is calculated using the following equation, Eq. (14):

$$\Delta G^\circ = -RT \ln K \tag{14}$$

where R is the universal gas constant (8.314 J (mol^{-1} K^{-1})), T is the absolute temperature in K and K (L g^{-1}) is an equilibrium constant obtained by multiplying the Langmuir constants Q_m and K_l [11].

The enthalpy (ΔH°) and entropy (ΔS°) parameters were estimated from the following equation:

$$\Delta G^\circ = \Delta H^\circ - T\Delta S^\circ \tag{15}$$

From Eqs. (14) and (15), we obtain Eq. (16):

Table 5
Comparison of adsorption capacities of different biosorbents for Ni(II) and Co(II) removal from aqueous solution

Metal ion	Biosorbent	Adsorption capacity (mg g^{-1})	References
	Banana peel	6.8	[46]
Ni(II)	Cashewnut shell	18.86	[16]
	Hazelnut shell	10.1	[47]
	Black carrot residues	5.75	[48]
	Cork bark	4.11	[49]
	Teak leaves	17.81	Present study
Co(II)	Hemp fibres	7.5	[3]
	Lemon peel	22	[4]
	Coir pith	12.82	[50]
	Black carrot residues	5.35	[48]
	Teak leaves	29.48	Present study

$$\ln K = \frac{\Delta S^\circ}{R} - \frac{\Delta H^\circ}{RT} \quad (16)$$

The values of ΔH° and ΔS° were calculated from the slope and intercept of the plot of ln K versus $1/T$. From Table 4, it can be inferred that the negative values of ΔG° for both the ions indicate the feasibility and spontaneous nature of the adsorption process. The positive values of ΔH° ensures the endothermic nature of adsorption and the positive value of ΔS° indicates the increase in affinity of the adsorbent at the solid/solution interface during the adsorption of Ni(II) and Co(II) ions on TLP.

Further, a comparison has been made for the maximum uptake capacities of different biosorbents for the removal of Ni(II) and Co(II) ions and presented in Table 5. It can be noted from the table that TLP shows good potential in removing nickel and cobalt ions from aqueous solution.

4. Conclusion

The results obtained from the batch study revealed that each of the process parameter, viz. initial pH, adsorbent dose, initial metal ion concentration, contact time and temperature have pronounced effect on the adsorption process. The maximum adsorption capacity of TLP for Ni(II) and Co(II) ions was found to be 17.81 and 29.48 mg g^{-1}, respectively. Kinetic studies revealed that the adsorption of both the metal ions could be described more favourably by the pseudo-second-order kinetic model. The Langmuir model provided the best representation of equilibrium data for both the metal ions. Moreover, the thermodynamic studies revealed that the process is feasible, endothermic and spontaneous in nature. Based on the results, it can be concluded that TLP can be effectively utilized as a natural adsorbent for the removal of nickel and cobalt ions from aqueous solution.

Acknowledgement

The authors would like to thank the Sophisticated Analytical Instrument Facility (SAIF), IIT Madras, Chennai for providing instrumental facility to carry out the SEM analysis. The authors would also like to thank the Department of Chemistry, IIT Madras, Chennai for providing facility to carry out the BET surface area analysis.

References

[1] L. Huang, Y. Sun, T. Yang, L. Li, Adsorption behavior of Ni(II) on lotus stalks derived active carbon by phosphoric acid activation, Desalination 268 (2011) 12–19.
[2] USEPA, Nickel Compounds Technology Transfer Network Air Toxics Web Site USEPA. Available from: http://www.epa.gov/ttn/atw/hlthef/nickel.html. Accessed 01-Dec-2013.
[3] M. Abbas, S. Kaddour, M. Trari, Kinetic and equilibrium studies of cobalt adsorption on apricot stone activated carbon, J. Ind. Eng. Chem. 20 (2014) 745–751.
[4] A. Shafaei, E. Pajootan, M. Nikazar, M. Arami, Removal of Co(II) from aqueous solution by electrocoagulation process using aluminum electrodes, Desalination 279 (2011) 121–126.
[5] D.M. Veneu, G.A.H. Pino, M.L. Torem, T.D. Saint'-Pierre, Biosorptive removal of cadmium from aqueous solutions using a *Streptomyces lunalinharesii* strain, Miner. Eng., 29 (2012) 112–120.
[6] E. Njikam, S. Schiewer, Optimization and kinetic modeling of cadmium desorption from citrus peels: A process for biosorbent regeneration, J. Hazard. Mater. 213–214 (2012) 242–248.
[7] D. Sud, G. Mahajan, M.P. Kaur, Agricultural waste material as potential adsorbent for sequestering heavy metal ions from aqueous solutions—A review, Bioresour. Technol. 99 (2008) 6017–6027.
[8] R.E. Wing, Starch citrate: Preparation and ion exchange properties, Starch Starke 48 (1996) 275–279.
[9] Y. Ding, D. Jing, H. Gong, L. Zhou, X. Yang, Biosorption of aquatic cadmium(II) by unmodified rice straw, Bioresour. Technol. 114 (2012) 20–25.
[10] S. Chen, Q. Yue, B. Gao, Q. Li, X. Xu, Removal of Cr (VI) from aqueous solution using modified corn stalks: Characteristic, equilibrium, kinetic and thermodynamic study, Chem. Eng. J. 168 (2011) 909–917.
[11] D.H.K. Reddy, D.K.V. Ramana, K. Seshaiah, A.V.R. Reddy, Biosorption of Ni(II) from aqueous phase by *Moringa oleifera* bark, a low cost biosorbent, Desalination 268 (2011) 150–157.
[12] A. Ahmadpour, M. Tahmasbi, T.R. Bastami, J.A. Besharati, Rapid removal of cobalt ion from aqueous solutions by almond green hull, J. Hazard. Mater. 166 (2009) 925–930.
[13] A. Bhatnagar, A.K. Minocha, Biosorption optimization of nickel removal from water using *Punica granatum* peel waste, Colloids Surf. B 76 (2010) 544–548.
[14] H. Hasar, Adsorption of nickel(II) from aqueous solution onto activated carbon prepared from almond husk, J. Hazard. Mater. 97 (2003) 49–57.
[15] A. Thevannan, R. Mungroo, C.H. Niu, Biosorption of nickel with barley straw, Bioresour. Technol. 101 (2010) 1776–1780.
[16] P.S. Kumar, S. Ramalingam, S.D. Kirupha, A. Murugesan, T. Vidhyadevi, S. Sivanesan, Adsorption behavior of nickel(II) onto cashew nut shell: Equilibrium, thermodynamics, kinetics, mechanism and process design, Chem. Eng. J. 167 (2011) 122–131.
[17] M.N. Zafar, R. Nadeem, M.A. Hanif, Biosorption of nickel from protonated rice bran, J. Hazard. Mater. 143 (2007) 478–485.
[18] R. Lakshmipathy, N.C. Sarada, Application of watermelon rind as adsorbent for removal of nickel and cobalt from aqueous solution, Int. J. Miner. Process. 122 (2013) 63–65.
[19] K.A. Krishnan, T.S. Anirudhan, Kinetic and equilibrium modelling of cobalt(II) adsorption onto bagasse

pith based sulphurised activated carbon, Chem. Eng. J. 137 (2008) 257–264.
[20] I.G. Shibi, T.S. Anirudhan, Kinetic and equilibrium modelling of adsorption of cobalt (II) from aqueous solutions onto surface modified lignocellulosics (*Musa paradisiaca*), Indian J. Chem. Technol. 13 (2006) 567–575.
[21] L. Tofan, C. Teodosiu, C. Paduraru, R. Wenkert, Cobalt (II) removal from aqueous solutions by natural hemp fibers: Batch and fixed-bed column studies, Appl. Surf. Sci. 285 (2013) 33–39.
[22] A. Bhatnagar, A.K. Minocha, M. Sillanpää, Adsorptive removal of cobalt from aqueous solution by utilizing lemon peel as biosorbent, Biochem. Eng. J. 48 (2010) 181–186.
[23] K.S. Rao, S. Anand, P. Venkateswarlu, Adsorption of cadmium(II) ions from aqueous solution by *Tectona grandis* L.f. (teak leaves powder), Bioresources 5 (2010) 438–454.
[24] S. Brunauer, P.H. Emmett, E. Teller, Adsorption of gases in multimolecular layers, J. Am. Chem. Soc. 60 (1938) 309–319.
[25] X. Luo, Z. Deng, X. Lin, C. Zhang, Fixed-bed column study for Cu^{2+} removal from solution using expanding rice husk, J. Hazard. Mater. 187 (2011) 182–189.
[26] K.S. Tong, M.J. Kassim, A. Azraa, Adsorption of copper ion from its aqueous solution by a novel biosorbent *Uncaria gambir*: Equilibrium, kinetics, and thermodynamic studies, Chem. Eng. J. 170 (2011) 145–153.
[27] D.L. Pavia, G.M. Lampman, G.S. Kriz, Introduction to Spectroscopy, third ed., Thomson Asia Pte. Ltd., Singapore, 2004.
[28] B. Singha, S.K. Das, Biosorption of Cr(VI) ions from aqueous solutions: Kinetics, equilibrium, thermodynamics and desorption studies, Colloids Surf. B 84 (2011) 221–232.
[29] H. Pahlavanzadeh, A.R. Keshtkar, J. Safdari, Z. Abadi, Biosorption of nickel(II) from aqueous solution by brown algae: Equilibrium, dynamic and thermodynamic studies, J. Hazard. Mater. 175 (2010) 304–310.
[30] S. Karthikeyan, R. Balasubramanian, C.S.P. Iyer, Evaluation of the marine algae *Ulva fasciata* and *Sargassum* sp. for the biosorption of Cu(II) from aqueous solutions, Bioresour. Technol. 98 (2007) 452–455.
[31] A. Olgun, N. Atar, Removal of copper and cobalt from aqueous solution onto waste containing boron impurity, Chem. Eng. J. 167 (2011) 140–147.
[32] A. Eser, V. Nüket Tirtom, T. Aydemir, S. Becerik, A. Dinçer, Removal of nickel(II) ions by histidine modified chitosan beads, Chem. Eng. J. 210 (2012) 590–596.
[33] M. Jain, V.K. Garg, K. Kadirvelu, Adsorption of hexavalent chromium from aqueous medium onto carbonaceous adsorbents prepared from waste biomass, J. Environ. Manage. 91 (2010) 949–957.
[34] A. Chatterjee, S. Schiewer, Multi-resistance kinetic models for biosorption of Cd by raw and immobilized citrus peels in batch and packed-bed columns, Chem. Eng. J. 244 (2014) 105–116.
[35] X. Pan, J. Wang, D. Zhang, Adsorption of cobalt to bone char: Kinetics, competitive adsorption and mechanism, Desalination 249 (2009) 609–614.
[36] Y. Ho, G. McKay, Pseudo-second-order model for adsorption processes, Process Biochem. 34 (1999) 451–465.
[37] M.I. El-Khaiary, G.F. Malash, Y.S. Ho, On the use of linearized pseudo-second-order kinetic equations for modeling adsorption systems, Desalination 257 (2010) 93–101.
[38] S. Chen, Q. Yue, B. Gao, X. Xu, Equilibrium and kinetic adsorption study of the adsorptive removal of Cr(VI) using modified wheat residue, J. Colloid Interface Sci. 349 (2010) 256–264.
[39] J.H. Chen, J.C. Ni, Q.L. Liu, S.X. Li, Adsorption behavior of Cd(II) ions on humic acid-immobilized sodium alginate and hydroxyl ethyl cellulose blending porous composite membrane adsorbent, Desalination 285 (2012) 54–61.
[40] A.E. Nemr, Potential of pomegranate husk carbon for Cr(VI) removal from wastewater: Kinetic and isotherm studies, J. Hazard. Mater. 161 (2009) 132–141.
[41] I. Langmuir, The adsorption of gases on plane surfaces of glass, mica and platinum, J. Am. Chem. Soc. 40 (1918) 1361–1403.
[42] T.W. Weber, R.K. Chakravorti, Pore and solid diffusion models for fixed-bed adsorbers, AIChE J. 20 (1974) 228–238.
[43] M. Jiang, X. Jin, X.-Q. Lu, Z. Chen, Adsorption of Pb (II), Cd(II), Ni(II) and Cu(II) onto natural kaolinite clay, Desalination 252 (2010) 33–39.
[44] J. Febrianto, A.N. Kosasih, J. Sunarso, Y.H. Ju, N. Indraswati, S. Ismadji, Equilibrium and kinetic studies in adsorption of heavy metals using biosorbent: A summary of recent studies, J. Hazard. Mater. 162 (2009) 616–645.
[45] A.M. Lazarin, C. Airoldi, Thermodynamics of the nickel and cobalt removal from aqueous solution by layered crystalline organofunctionalized barium phosphate, J. Chem. Thermodyn. 41 (2009) 21–25.
[46] G. Annadural, R.S. Juang, D.J. Lee, Adsorption of heavy metals from water using banana and orange peels, Water Sci. Technol. 47 (2003) 185–190.
[47] E. Demirbas, M. Kobya, S. Oncel, S. Sencan, Removal of Ni(II) from aqueous solution by adsorption onto hazelnut shell activated carbon: Equilibrium studies, Bioresour. Technol. 84 (2002) 291–293.
[48] F. Guzel, H. Yakut, G. Topal, Determination of kinetic and equilibrium parameters of the batch adsorption of Mn(II), Co(II), Ni(II) and Cu(II) from aqueous solution by black carrot (*Daucus carota L.*) residues, J. Hazard. Mater. 153 (2008) 1275–1287.
[49] B. Southichak, K. Nakano, M. Nomura, N. Chiba, *Phragmites australis*: A novel biosorbent for the removal of heavy metals from aqueous solution, Water Res. 40 (2006) 2295–2302.
[50] H. Parab, S. Joshi, N. Shenoy, A. Lali, U.S. Sarma, M. Sudersanan, Determination of kinetic and equilibrium parameters of the batch adsorption of Co(II), Cr(III) and Ni(II) onto coir pith, Process Biochem. 41 (2006) 609–615.